HAL
archives-ouvertes.fr

Activation of Lung p53 by Nutlin-3a Prevents and Reverses Experimental Pulmonary Hypertension.

Nathalie Mouraret, Elisabeth Marcos, Shariq Abid, Guillaume Gary-Bobo, Mirna Saker, Amal Houssaini, Jean-Luc Dubois-Rande, Laurent Boyer, Jorge Boczkowski, Geneviève Derumeaux, et al.

▶ **To cite this version:**

Nathalie Mouraret, Elisabeth Marcos, Shariq Abid, Guillaume Gary-Bobo, Mirna Saker, et al.. Activation of Lung p53 by Nutlin-3a Prevents and Reverses Experimental Pulmonary Hypertension.. Circulation, American Heart Association, 2013, 127 (16), pp.1664-76. 10.1161/CIRCULATIONAHA.113.002434 . inserm-00829264

HAL Id: inserm-00829264
https://www.hal.inserm.fr/inserm-00829264

Submitted on 1 Sep 2013

HAL is a multi-disciplinary open access archive for the deposit and dissemination of scientific research documents, whether they are published or not. The documents may come from teaching and research institutions in France or abroad, or from public or private research centers.

L'archive ouverte pluridisciplinaire **HAL**, est destinée au dépôt et à la diffusion de documents scientifiques de niveau recherche, publiés ou non, émanant des établissements d'enseignement et de recherche français ou étrangers, des laboratoires publics ou privés.

Activation of Lung p53 by Nutlin-3a Prevents and Reverses Experimental Pulmonary Hypertension

Mouraret; Role of Cell Senescence in Pulmonary Hypertension

Mouraret N MSC*, Marcos E MSC*, Abid S MSC*, Gary-Bobo G PhD*, Saker M MSC*, Houssaini A MSC*, Dubois-Rande JL MD‡, Boyer L MD*, Boczkowski J MD-PhD*, Derumeaux G MD †, Amsellem V PhD*, Adnot S MD-PhD*

* INSERM U955 and Département de Physiologie, Hôpital Henri Mondor, AP-HP, 94010, Créteil, France, Université Paris-Est Creteil (UPEC), France

‡ Service de Cardiologie, Hôpital Henri Mondor, AP-HP, 94010, Créteil, France, Université Paris-Est Creteil (UPEC), France

† CarMeN INSERM Unit 1060, Université de Lyon, Lyon, France

Correspondence: Serge Adnot, Hôpital Henri Mondor, Service de Physiologie-Explorations Fonctionnelles, 94010, Créteil, France

E-mail: **serge.adnot@inserm.fr**; Tel: +33 149 812 677; Fax: +33 149 812 667

Word count: 6979

Subject codes:

[162] Smooth muscle proliferation and differentiation

[18] Pulmonary circulation and disease

[115] Remodeling

ABSTRACT

Background: Induction of cellular senescence through activation of the p53 tumor suppressor protein is a new option for treating proliferative disorders. Nutlins prevent the ubiquitin ligase MDM2 (murine double minute 2), a negative p53 regulator, from interacting with p53. We hypothesized that cell senescence induced by Nutlin-3a exerted therapeutic effects in pulmonary hypertension (PH) by limiting the proliferation of pulmonary-artery smooth muscle cells (PA-SMCs).

Methods and results: Nutlin-3a treatment of cultured human PA-SMCs resulted in cell growth arrest with the induction of senescence but not apoptosis; increased phosphorylated p53 protein levels; and expression of p53 target genes including p21, Bax, BTG2, and MDM2. Daily intraperitoneal Nutlin-3a treatment for 3 weeks dose-dependently reduced PH, right ventricular hypertrophy, and distal pulmonary artery muscularization in mice exposed to chronic hypoxia or SU5416/hypoxia. Nutlin-3a treatment also partially reversed PH in chronically hypoxic or transgenic mice overexpressing the serotonin-transporter in SMCs (SM22-5HTT+ mice). In these mouse models of PH, Nutlin-3a markedly increased senescent p21-stained PA-SMCs; lung p53, p21, and MDM2 protein levels; and p21, Bax, PUMA, BTG2, and MDM2 mRNA levels; but induced only minor changes in control mice without PH. Marked MDM2 immunostaining was seen in both mouse and human remodeled pulmonary vessels, supporting the use of Nutlins as a PH-targeted therapy. PH prevention or reversal by Nutlin-3a required lung p53 stabilization and increased p21 expression, as indicated by the absence of Nutlin-3a effects in hypoxia-exposed $p53^{-/-}$ and $p21^{-/-}$ mice.

Conclusion: Nutlin-3a may hold promise as a prosenescence treatment targeting PA-SMCs in PH.

Keywords: hypertension, pulmonary; cell senescence; muscle; remodeling

INTRODUCTION

Pulmonary artery hypertension (PH) occurring as an idiopathic condition or associated with an underlying disease is an unexplained disorder whose severe forms in adults and neonates are fatal and for which no satisfactory treatment is available. Hyperplasia of pulmonary-artery smooth muscle cells (PA-SMCs) is the primary determinant of the pulmonary vessel remodeling process that underlies PH[1]. Similarities exist between cancer and PH. Thus, cultured PA-SMCs and pulmonary-artery endothelial cells (PA-ECs) from patients with PH show growth dysregulation[2-5], PA-SMCs from patients with PH have decreased susceptibility to apoptosis[6], remodeled pulmonary vessels express cancer biomarkers[7], and drugs designed to treat malignant proliferations exert beneficial effects in animal models of PH[8].

One common abnormality in cancer is an inactivating mutation in the gene encoding the powerful growth-suppressive and proapoptotic transcription factor p53[9]. Also common is posttranslational p53 inactivation via interaction of the p53 protein with its negative regulator MDM2 (murine double minute 2), a specific p53 ubiquitin ligase and transcriptional inhibitor[10, 11]. MDM2 is overexpressed in many human tumors, suggesting that p53-MDM2 interactions may hold promise as a target for cancer therapy[12]. Nutlins are cis-imidazoline analogs recently developed as anticancer agents[13]. These selective small-molecule p53-MDM2 binding inhibitors stabilize p53, thereby increasing the expression of genes targeted by p53 including the antiproliferative gene BTG2, the prosenescent gene p21, and the proapoptotic genes Bax and PUMA[14]. The most potent Nutlin, Nutlin-3a, exhibits antitumor activity via p53 activation in various cancer cells and induces tumor regression when administered chronically to mice[13]. Nutlin-3a is being tested for the treatment of lymphoblastic leukemia in humans[15].

Treatments that activate p53 in PA-SMCs might be capable of limiting or reversing the pulmonary vascular remodeling process that characterizes PH. The ability of Nutlin-3a to stabilize and activate p53 in target cells depends on the expression and/or activity of MDM2 in these cells. MDM2 dysregulation has been reported in SMCs at sites of vascular injury[16], as well as in human atherosclerotic tissues and in vascular SMCs from patients with primary aldosteronism[17, 18]. Moreover, MDM2 expression can be induced by hypoxia or by p53[11, 19]. Whether MDM2 expression or activity is altered during progression of hypoxic or nonhypoxic PH remains unexplored. The potential effects of p53 activation in target cells may also vary according to cell status or environmental conditions, leading to cell quiescence, senescence, or apoptosis[20-23]. Both senescence and apoptosis of PA-SMCs may provide therapeutic benefits in PH, although the accumulation of senescent cells within the vessel wall may potentially affect the remodeling process[24]. Until now, prosenescence therapy for PH has not been evaluated.

In the present study, we tested the hypothesis that Nutlins hold therapeutic potential in PH via prosenescence effects. To this end, we first examined the effects of Nutlin-3a on cultured human PA-SMCs. Second, we investigated the effects of chronic Nutlin-3a treatment in normoxic mice free of PH; mice with hypoxia-induced PH; chronically hypoxic mice simultaneously treated with SU5416 (SU5416/hypoxia)[25]; and transgenic mice overexpressing the serotonin transporter in SMCs (SM22-5HTT+ mice), which develop spontaneous PH in normoxia[26]. Finally, we examined the mechanisms of action of Nutlin-3a by investigating p53 and p21 knockout mice exposed to chronic hypoxia.

MATERIALS AND METHODS

Mice

Adult male mice (C57Bl/6j) were used according to institutional guidelines that complied with national and international regulations. All animal experiments were approved by the Institutional Animal Care and Use Committee of the French National Institute of Health and Medical Research (INSERM)-Unit 955, Créteil, France. Transgenic mice overexpressing 5-HTT in smooth muscle cells (SMCs) under the control of the SM22 promoter (SM22-5HTT+) were produced and bred as previously described[26]. These SM22-5HTT+ mice are fertile and have a normal life span and normal growth[5]. Mice with deletion of the p53 ($p53^{-/-}$) or p21 ($p21^{-/-}$) gene were obtained from Jackson Laboratory (Bar Harbor, ME). Only male mice were used for the experiments. Nutlin-3a was administered by intraperitoneal injection in a dosage of 6, 12, or 25 mg/Kg/day. At treatment completion, the lungs were removed and prepared for histological or Western-blot analyses.

Exposure to chronic hypoxia

Male mice aged 15-20 weeks were exposed to chronic hypoxia (9% O_2) in a ventilated chamber (Biospherix, New York, NY) [27]. To establish the hypoxic environment, the chamber was flushed with a mixture of room air and nitrogen. The chamber was opened every other day for 1 hour to clean the cages, administer drugs, and replenish food and water supplies. Normoxic mice were kept in the same room, with the same light-dark cycle. Mice subjected to SU5416/hypoxia received an intraperitoneal injection of SU5416 20 mg/Kg once a week during a 3-week period of hypoxia exposure [25].

Assessment of pulmonary hypertension

We anesthetized mice previously exposed to hypoxia, room air, or SU5416/hypoxia; as well as SM22-5HTT+ mice. After incision of the abdomen, a 26-gauge needle connected to a pressure transducer was inserted into the right ventricle through the diaphragm, and right ventricular systolic pressure (RVSP) was recorded immediately. Then, the thorax was opened and the lungs and heart were removed. The right ventricle (RV) was dissected from the left ventricle plus septum (LV+S), and these dissected samples were weighed for determination of Fulton's index (RV/LV+S). The lungs were fixed by intratracheal infusion of 4% aqueous buffered formalin. A midsagittal slice of the right lung was processed for paraffin embedding. Sections 5 µm in thickness were cut and stained with hematoxylin-phloxine-saffron for examination by light microscopy. In each mouse, a total of 20 to 30 intraacinar vessels accompanying either alveolar ducts or alveoli were examined by an observer who was blinded to the treatment or genotype. Each vessel was categorized as nonmuscular (no evidence of vessel wall muscularization) or muscular, i.e., partially muscular (SMCs identifiable in less than three-fourths of the vessel circumference) or fully muscular (SMCs in more than three-fourths of the vessel circumference). The percentage of muscularized pulmonary vessels was determined by dividing the number of partially or fully muscular vessels by the total number of vessels in the relevant group of animals. In addition, medial wall thickness of fully muscularized intraacinar arteries was calculated in SU5416/hypoxia mice and expressed as follows: index (%)=(external diameter - internal diameter)/external diameter·100. Cell proliferation (Ki67-stained cells), apoptosis (TUNEL-positive cells), and senescence (p21-stained cells) were assessed in the walls of distal pulmonary vessels and expressed as the number of stained nuclei over the total number of nuclei counted in the media of at least 20 muscularized vessels per mouse.

Echocardiography

Closed-chest transthoracic echocardiography was performed in nonsedated mice as described in the expanded methods section available in the Online Supplement. Images were acquired using a 13-MHz linear-array transducer with a digital ultrasound system (Vivid 7, GE Medical Systems). All measures were averaged on 5 cardiac cycles, and the reader was blinded to treatment group.

Studies on cultured human pulmonary artery smooth muscle cells (PA-SMCs)

Cultured PA-SMCs were collected from pulmonary arteries of patients undergoing lung surgery for localized lung tumors[24]. To assess the effects of Nutlin-3a on PA-SMC proliferation, we exposed PA-SMCs to Nutlin-3a (2.5-10 μM) or vehicle in serum-free medium then added platelet-derived growth factor-BB (PDGF-BB, 50 ng/mL). After 48 hours, tetrazolium salt (MTT, Sigma, Lyon, France) was added to each well (0.2 mg/mL). After 4 hours' incubation at 37°C, the culture medium was removed and formazan crystals were solubilized by adding 500 μL of DMSO. Tetrazolium salt reduction to formazan within the cells was quantified by spectrophotometry at 520 nm and taken as an indicator of the number of cells.

To assess the effects of Nutlin-3a on PA-SMC apoptosis, cells were trypsinized and resuspended in binding buffer 1X then incubated with annexin V-FITC–conjugated antibody and stained with propidium iodide according to the manufacturer's instructions (Sigma-Aldrich, St Louis, MO). Annexin V staining and propidium iodide staining were detected by FACS (Becton Dickinson, Franklin Lakes, NJ). Apoptotic cells were propidium iodide-positive cells and annexin V/propidium iodide-positive cells.

To assess the effects of Nutlin-3a on cell senescence, we determined the percentage of beta-galactosidase (β-gal)-positive cells after 48 hours' incubation with Nutlin-3a with or without vehicle or platelet-derived growth factor (PDGF).

In addition, cell transfection studies were performed using a p53 Cignal Reporter Assay (Qiagen, ZA Courtaboeuf, France) for assessing p53 signaling in response to Nutlin, as described in the online supplement.

Biological measurements in mouse tissues and cultured human pulmonary-artery smooth muscle cells (PA-SMCs)

Western blotting was used to detect and quantitate p53, p21 and MDM2 proteins in mouse tissues and/or human cells as described in the expanded methods section in the Online Supplement. Complementary experiments were performed in mouse tissue to assess phosphorylated p53 levels by using a co-immunoprecipitation procedure or to determine the nuclear and cytoplasmic fractions of total p53 protein. Levels of p21, Bax and PUMA mRNAs in lung tissue and cells were determined using RT-qPCR. Total mRNA was extracted from PA-SMCs using the RNeasy Mini Kit (Qiagen, ZA Courtaboeuf, France). First-strand cDNA was synthesized in reversed transcribed samples, as follows: 1 µg total RNA isolated from cells or lung tissues, 200 U/µL SuperScript II reverse transcriptase, 100 ng Random primers, and 10 mM mixed dNTP (Invitrogen, Life Technologies, Cergy-Pontoise, France). Quantitative PCR was performed in a 7900HT Real-Time PCR system (Applied Biosystems, ZA Courtaboeuf, France), using SYBR green Mix from Invitrogen as described in the expanded methods section in the Online Supplement.

Immunohistochemistry

Paraffin-embedded sections were incubated with antibodies against Ki67 or p21 for immunostaining identification of vascular proliferative or senescent cells, respectively. Apoptotic nuclei were labeled with a TUNEL immunostaining assay (Roche, Meylan, France), as described in the expanded Methods section available in the Online Supplement. For immunofluorescence, slides were incubated with anti-MDM2 SMP-14 mouse antibody (1:50, Santa Cruz, Santa Cruz, CA) and anti-αSMA rabbit antibody (1:200, Abcam, Cambridge, UK) then exposed to anti-mouse Alexa Fluor (1:1000, Cell Signaling Technology, Boston, MA) and anti-rabbit Alexa Fluor (1:1000, Invitrogen, Cergy-Pontoise, France) antibodies. Nuclei were stained with Hoechst 333342 (1 μg/mL, Cell Signaling Technology).

Chemicals and drugs

Nutlin-3a was purchased from Bertin Pharma (Montigny-le-Bretonneux, France) and diluted in vehicle (0.9% NaCl and 30% DMSO) to obtain concentrations of 6 mg/Kg, 12 mg/Kg, and 25 mg/Kg. Mice received daily intraperitoneal injections of Nutlin-3a for 21 days. SU5416 was purchased from Sigma (Saint Quentin Fallavier, France).

Statistical analysis

The data are described as mean±SEM. Parametric tests were used after verification that the variables in each group were normally distributed. One-way analysis of variance (ANOVA) was performed to compare treatment effects with the three Nutlin-3a doses and the vehicle. When a significant difference was found, group means were compared using the modified *t* test. *P* values lower than 0.05 were considered significant.

RESULTS

Effects of Nutlin-3a treatment on cultured human PA-SMCs

Nutlin-3a treatment of cultured human PA-SMCs was followed by a marked rise in phosphorylated p53 protein levels within 2 hours after treatment, with a peak after 4 hours and persistent elevation until 24 hours (Figure 1A); total p53 protein and p53 mRNA levels remained unchanged (Figure 1A). Nutlin-3a treatment also induced marked but delayed increases in p21 mRNA and protein levels, which peaked at 24 hours (Figure 1B) and were accompanied with increased expression of other p53-target genes including Bax, BTG2 and MDM2 (data not shown). After 24 hours of Nutlin-3a treatment, β-galactosidase-stained cells increased in percentage from 20% to 90% and exhibited a typical senescent phenotype characterized by a flat shape and increased size, in the absence or presence of PDGF (Figures 1C and 1D). The number of annexin-V-positive cells was not affected by Nutlin-3a (Figure 1C). Nutlin-3a treatment dose-dependently increased the phosphorylated p53 protein and p21 protein levels without altering the caspase-3 protein level (Figure 1E), indicating that Nutlin-3a treatment induced senescence but not apoptosis of PA-SMCs. In addition, Nutlin-3a applied to cells transfected with the luciferase p53 reporter, led to a marked increase in luciferase activity compared with vehicle-treated control cells (Figure 1F).

Effects of treatment with Nutlin-3a in mice exposed to chronic hypoxia

Intraperitoneal treatment of chronically hypoxic mice with 6 to 25 mg/Kg/day of Nutlin-3a attenuated the development of PH, as judged based on RVSP, RV hypertrophy, and distal pulmonary artery muscularization (Figure 2A). This protective effect of Nutlin-3a was accompanied with simultaneous decreases in PA-SMC proliferation and apoptosis, as assessed by the percentage of Ki67- and TUNEL-positive cells, respectively, contrasting with

an increased number of senescent p21-positive PA-SMCs (Figures 2A and 2B). Cardiac output and left ventricular ejection fraction remained unchanged in mice treated with 25 mg/Kg/day of Nutlin-3a, whereas pulmonary acceleration time (PAT) and the PAT/ejection time ratio, two alternative indices of pulmonary artery pressure, improved in chronically hypoxic mice (Online Table I). Nutlin-3a, 12 mg/Kg/d, from day 15 to day 30 partially reversed PH in chronically hypoxic mice (Figure 2C).

Nutlin-3a treatment markedly increased lung levels of p53, p21, and MDM2 protein and of p21, Bax, Bcl2, and BTG2 mRNAs in chronically hypoxic mice but not in normoxic animals (Figures 3A and 3D). Phosphorylated p53 protein levels measured in whole lung proteins and total p53 protein levels measured in the nuclear and cytoplasmic fractions of lung proteins increased after Nutlin-3a treatment in hypoxic but not normoxic mice (Figure 3B 3C). Because lung samples were collected exactly 3 hours after the last Nutlin-3a injection in both normoxic and hypoxic mice, the dissimilar response to Nutlin-3a in hypoxic and normoxic mice was interpreted as reflecting increased MDM2 activity during hypoxia. This increased MDM2 activity was measured, although total lung MDM2 protein levels did not change from normoxia to hypoxia (Figure 3A). In contrast to the dose-dependent increase in lung p21, Bax, Bcl2, and BTG2 mRNA levels induced by Nutlin-3a, lung expression of the proapoptotic gene PUMA, which increased from normoxia to hypoxia, was reduced by Nutlin-3a treatment (Figure 3D). The increased p53 protein levels induced by Nutlin-3a also occurred in the kidneys, heart, spleen, and liver from normoxic and hypoxic mice, although at different levels (online Figure 1). A marked (3.5-fold) increase in p53 protein was observed only in the lungs and kidneys of chronically hypoxic mice.

Effects of Nutlin-3a treatment in SM22-5HTT^{+} mice and in SU5416/hypoxia mice

SM22-5-HTT+ mice were studied to investigate whether Nutlin-3a reversed established PH and altered MDM2 activity during normoxia. SM22-5HTT^{+} mice, which spontaneously develop PH, were treated for 3 weeks with 12 mg/Kg/day Nutlin-3a. Nutlin-3a partially reversed PH in SM22-5-HTT^{+} mice, decreasing RVSP, RV hypertrophy, pulmonary vessel muscularization, and Ki67-stained cell counts (Figure 4); and substantially increased p21-stained cell counts; without increasing TUNEL-positive cell counts. Similarly to the findings in chronically hypoxic mice, Nutlin-3a treatment increased lung p53, p21, and MDM2 protein levels; as well as mRNA levels of the p53-target genes p21, Bax, Bcl2, and BTG2 (Figures 5 and online Figure 2). Nutlin-3a also increased lung PUMA mRNA levels in SM22-5-HTT+ mice (online Figure 2). No such alterations were observed in wild-type mice, indicating increased lung MDM2 activity in SM225-HTT+ mice, similar to chronically hypoxic mice. In contrast to the results in chronically hypoxic mice, total lung p53, p21, and MDM2 protein levels were slightly higher in SM22-5-HTT+ mice than in wild-type mice and increased further in response to Nutlin-3a (Figure 5).

To assess the effects of Nutlin-3a in a third model of PH characterized by more intense pulmonary vascular remodeling, we investigated mice subjected to SU5416/hypoxia[25]. Treatment with 12 mg/Kg/d during 3 weeks partially prevented PH in SU5416/hypoxia mice, inducing a substantial increase in p21-stained cell counts and marked attenuation of the increased wall thickness of pulmonary vessels (online Figure 3A and 3B). MDM2 protein levels, which were higher in SU5416/hypoxia mice than in wild-type mice, increased further in response to Nutlin-3a (Online Figure 3C).

Immunolocalization of MDM2 in lung tissues from mice and patients with chronic lung disease

In both normoxic and chronically hypoxic mice, immunofluorescence staining for MDM2 protein was predominantly found in SMCs from the media of pulmonary vessels, as shown by double-immunofluorescence staining for MDM2 and αSMA of paraffin-embedded lung sections (Figure 6 A). Only a few MDM2-stained cells were observed in the bronchi and alveoli. Similar findings were obtained in SM22-5-HTT+ mice. In lung tissues from lung-surgery patients with or without pulmonary vessel remodeling, MDM2 also predominated in SMCs of pulmonary vessels (Figure 6 B).

Effects of treatment with Nutlin-3a in $p53^{-/-}$ mice

To determine whether Nutlin-3a effects required p53 stabilization, we investigated $p53^{-/-}$ mice and their littermate controls during exposure to chronic hypoxia. Nutlin-3a in a dose of 12 mg/Kg/day did not prevent hypoxic PH in $p53^{-/-}$ mice, in contrast to its protective effect in control nonmutant mice (Figure 7A). Nutlin-3a treatment also failed to alter p53 downstream signaling in these mice, indicating clearly that p53 was required to mediate Nutlin-3a effects (Figures 7B and online Figure 4). Interestingly, PH was slightly but significantly more severe in $p53^{-/-}$ mice than in control wild-type mice, in accordance with previously published studies[28].

Effects of treatment with Nutlin-3a in $p21^{-/-}$ mice

To determine whether p21 was required to prevent PH in chronically hypoxic mice, we investigated the effects of Nutlin-3a treatment in $p21^{-/-}$ mice. As shown in Figure 8, Nutlin-3a treatment failed to protect hypoxia-exposed $p21^{-/-}$ mice against PH. Interestingly, the ability of Nutlin-3a treatment to enhance Bax and BTG2 expression was reduced but not abrogated in $p21^{-/-}$ mice, whereas Nutlin-3a-induced changes in Bcl2 and PUMA expression were

abolished (online Figure 5). In $p21^{-/-}$ mice, PH was slightly but significantly more severe than in wild-type controls, suggesting that p21-induced cell senescence not only was critical in mediating Nutlin-3a effects, but also played a role in the development of hypoxic PH.

DISCUSSION

The main finding of the present study is that Nutlin-3a, a potent and selective antagonist of the p53-MDM2 interaction, induces PA-SMC senescence in vitro and attenuates or reverses PH in three distinct experimental mouse models, decreasing the number of proliferating PA-SMCs and increasing the number of p21-stained senescent cells. Nutlin-3a led to marked increases in lung p53 protein and p53 downstream gene expression in mice with PH, whereas only minor effects were noted in control mice without PH. These results are consistent with potentiation of Nutlin-3a effects in PH due to increased MDM2 activity. The ability of Nutlin-3a to prevent or reverse PH required lung p53 stabilization and increased p21 expression, as indicated by the inability of Nutlin-3a to prevent chronic hypoxia-induced PH in $p53^{-/-}$ and $p21^{-/-}$ mice. Thus, Nutlin-3a holds promise as a prosenescence treatment targeting PA-SMCs during PH progression.

The induction of cell senescence is a novel therapeutic approach to malignant and nonmalignant proliferative disorders[29]. Inducing PA-SMC senescence is expected to be more efficient than inducing cell quiescence in PH, as cell growth arrest in senescence is stable and largely irreversible. Here, we found that Nutlin-3a treatment of human PA-SMCs led to a large increase in phosphorylated p53 protein levels, with a subsequent increase in p21 expression and acquisition of a typical senescence phenotype characterized by increased size, a flat shape, and β-gal staining. This senescence-induced growth arrest appeared irreversible, since Nutlin-3a removal did not restore PA-SMC proliferation. However, PA-SMCs treated with Nutlin-3a did not become apoptotic, a finding consistent with results obtained using other cell types, including fibroblasts from mice and humans[20, 21].

Chronic Nutlin-3a treatment of mice during hypoxia exposure considerably attenuated PH severity by decreasing distal pulmonary artery muscularization. This effect was dose-

dependent, and no toxic effects were detected even at the highest dose tested. Nutlin-3a treatment for 3 weeks also attenuated PH in mice subjected to SU5416/hypoxia and partially reversed established PH in SM22-5HTT+ mice and in chronically hypoxic mice, producing similar decreases in pulmonary vessel muscularization. These effects of Nutlin-3a were associated with a marked reduction in Ki67-positive dividing PA-SMCs, together with an increased number of p21-stained PA-SMCs, but with no increase in apoptotic TUNEL-positive cells. Taken together with our in vitro data, these results indicate that prevention or reversal of pulmonary vessel remodeling in our mouse models of PH resulted from the induction of PA-SMC senescence by Nutlin-3a.

We found that the number of p21-stained senescent cells following Nutlin-3a treatment increased to a much greater extent in lungs from chronically hypoxic and SM22-5HTT+ mice than from their respective controls without PH, suggesting potentiation of Nutlin-3a effects during PH. One potential advantage of using Nutlin to treat cancer is that cancer cells overexpress MDM2 and should therefore prove more susceptible than normal cells to growth arrest in response to Nutlin[12, 23]. The results of the present study also suggest greater susceptibility to Nutlin-3a of proliferating PA-SMCs in PH, compared to PA-SMCs from control animals. Nutlin-3a administration was followed by considerably larger increases in lung p53 protein levels in chronically hypoxic mice and SM22-5HTT+ normoxic mice than in their respective controls. These effects were related to increased MDM2 activity in chronically hypoxic mice and to increased MDM2 activity and expression in SM22-5HTT+ mice. Potentiation of Nutlin-3a effects during PH was also supported by the Nutlin-3a-induced expression of p53 downstream genes including p21, Bax, Bcl2, BTG2, and MDM2, which was far greater in hypoxic and SM22-5HTT+ mice than in control mice without PH. Moreover, MDM2 was strongly expressed by PA-SMCs in remodeled vessels from

chronically hypoxic mice, from SM22-5HTT+ mice, and from mice subjected to SUGEN/hypoxia compared to those from mice without PH. PA-SMCs from remodeled pulmonary vessels of patients with chronic lung disease also exhibited increased MDM2 immunostaining compared to those from nonremodeled vessels of the same patients. Taken together, these results indicate that prevention or reversal of pulmonary vessel remodeling in these mouse models of PH was due to the induction of PA-SMC senescence and that the effects of Nutlin-3a on PA-SMCs were potentiated during PH, probably because of activation and/or overexpression of the Nutlin-3a target MDM2 protein. Thus, Nutlin-3a holds promise as a targeted treatment for PH.

Of note, we found that Nutlin-3a treatment increased both phosphorylated and nonphosphorylated p53 protein in lungs from hypoxic mice but increased only phosphorylated p53 protein in cultured human PA-SMCs. Neither phosphorylated nor total p53 protein was altered by Nutlin-3a in lungs from normoxic mice. These results are consistent with data suggesting that Nutlin-3a efficacy may vary according to basal MDM2 activity and conditions of Nutlin-3a treatment[29, 30]. Moreover they emphasize the complexity of the interactions between MDM2 and p53. Indeed, the MDM2-p53 complex is known to form primarily in the nucleus and to shuttle subsequently from the nucleus to the cytoplasm, where MDM2 targets p53 for degradation by acting as an ubiquitin-ligase[30]. The dissimilar effects of Nutlin-3a in hypoxic versus normoxic mice are also consistent with previous studies showing that systemic Nutlin treatment is toxic to tumor tissue but not to normal tissue [31, 32]. In both normoxic and hypoxic mice treated with Nutlin-3a, we observed minimal changes in p53 protein levels in the heart, spleen, and liver and found that cardiac function remained unaltered. Major increases in p53 protein were seen not only in the lungs, but also in the kidneys. Further studies are therefore needed to assess the renal effects of Nutlins in

conditions associated with PH, although Nutlins have been reported to improve kidney function in other conditions [33].

Although p53 regulation appears to be the central focus of MDM2 activity, the p53-binding domain of MDM2 binds to other proteins that are potentially involved in cell growth and survival[34]. To investigate whether Nutlin-3a effects were mediated solely by stabilization and overexpression of p53, we investigated $p53^{-/-}$ mice. Nutlin-3a did not prevent PH in $p53^{-/-}$ mice simultaneously exposed to chronic hypoxia. Neither did Nutlin-3a alter p53 downstream signaling in these mice, clearly indicating that p53 was required to mediate the effects of Nutlin-3a. Another point of interest was whether p53 played a pivotal role in PH development in our mouse models. As previously reported, we found that PH was more severe in $p53^{-/-}$ mice than in control wild-type mice[28]. However, in contrast to these previous studies showing marked increases in lung p53 protein levels from normoxia to hypoxia[28], we observed only minimal alterations in baseline p53 levels in hypoxic vs. normoxic mice and in SM22-5HTT+ mice vs. control wild-type mice. The reason for this difference is unclear but probably involves differences in hypoxia exposure conditions. The relative stability of p53 protein levels from normoxia to hypoxia in our study is probably ascribable to increased p53 protein degradation due to increased MDM2 ubiquitin ligase activity. Suppression of this adaptive response by Nutlin-3a led to major increases in p53 in PA-SMCs, thereby strongly inhibiting the pulmonary vascular remodeling process.

Among the transcriptional targets of p53, p21 has been shown to play a major role as a regulator of cell-cycle progression and to be involved in cell senescence [35]. We found that the protective action of Nutlin-3a against PH required p21, as indicated by the inability of Nutlin-3a to prevent chronic hypoxia-induced PH in $p21^{-/-}$ mice, despite significant increases in mRNA levels of the antiproliferative protein BTG2 and of the proapoptotic protein Bax.

These results indicate a prominent role for p21 in our experimental PH model and support cell-senescence induction as the mechanism by which Nutlin-3a protects against PH. Moreover, the slight increase in PH severity noted in $p21^{-/-}$ mice compared to their hypoxic controls suggests involvement of p21 in the control of hypoxic PH progression.

The present results supporting a beneficial effect of cell-senescence induction in PH may appear to contradict our previous studies supporting a role for senescent cells in mediating pulmonary vascular remodeling. In these previous studies, we showed that the accumulation of senescent cells within pulmonary vessels contributed to neointima formation in patients with chronic lung diseases[24]. Indeed, senescent cells are still metabolically active and release various factors including cytokines, growth factors, and matrix components; which promote the proliferation of neighboring cells[24, 35, 36]. Similar observations have been made for cancer cells, which can be stimulated by neighboring senescent cells [35]. Thus, an important issue regarding PH is whether senescent cells can accumulate for long periods in pulmonary vessels. In theory, such accumulation is prevented via senescent-cell clearance by the immune system[37]. However, in age-related diseases such as chronic obstructive lung disease, combined mechanisms, including increased susceptibility to cell senescence and an inability of the immune system to clear senescent cells, probably promote the accumulation of senescent cells within the vascular wall. Whether this may occur in response to Nutlin treatment may depend on various factors such as age, immune system performance, and environmental conditions[37]. Thus, inducing cell senescence might hold promise as a treatment against pulmonary vascular remodeling, provided the senescent cells are simultaneously cleared by the immune system.

Further studies are therefore needed to identify the mechanisms responsible for senescent-cell clearance in PH. Whether prosenescence strategies such as Nutlin therapy hold promise for the treatment of PH will need to be evaluated.

Funding sources

This study was supported by grants from the INSERM, Fondation pour la Recherche Médicale, Ministère de la Recherche, Chancellerie des universities de Paris, and Fondation Caresen.

Disclosures

The authors have no conflicts of interest to disclose.

References

1. Morrell NW, Adnot S, Archer SL, Dupuis J, Jones PL, MacLean MR, McMurtry IF, Stenmark KR, Thistlethwaite PA, Weissmann N, Yuan JX, Weir EK. Cellular and molecular basis of pulmonary arterial hypertension. *J Am Coll Cardiol.* 2009;54(1 Suppl):S20-31.

2. Eddahibi S, Humbert M, Fadel E, Raffestin B, Darmon M, Capron F, Simonneau G, Dartevelle P, Hamon M, Adnot S. Serotonin transporter overexpression is responsible for pulmonary artery smooth muscle hyperplasia in primary pulmonary hypertension. *J Clin Invest.* 2001;108(8):1141-1150.

3. Yeager ME, Halley GR, Golpon HA, Voelkel NF, Tuder RM. Microsatellite instability of endothelial cell growth and apoptosis genes within plexiform lesions in primary pulmonary hypertension. *Circ Res.* 2001;88(1):E2-E11.

4. Lee SD, Shroyer KR, Markham NE, Cool CD, Voelkel NF, Tuder RM. Monoclonal endothelial cell proliferation is present in primary but not secondary pulmonary hypertension. *J Clin Invest.* 1998;101(5):927-934.

5. Eddahibi S, Guignabert C, Barlier-Mur AM, Dewachter L, Fadel E, Dartevelle P, Humbert M, Simonneau G, Hanoun N, Saurini F, Hamon M, Adnot S. Cross talk between endothelial and smooth muscle cells in pulmonary hypertension: critical role for serotonin-induced smooth muscle hyperplasia. *Circulation.* 2006;113(15):1857-1864.

6. Atkinson C, Stewart S, Upton PD, Machado R, Thomson JR, Trembath RC, Morrell NW. Primary pulmonary hypertension is associated with reduced pulmonary vascular expression of type II bone morphogenetic protein receptor. *Circulation.* 2002;105(14):1672-1678.

7. McMurtry MS, Archer SL, Altieri DC, Bonnet S, Haromy A, Harry G, Puttagunta L, Michelakis ED. Gene therapy targeting survivin selectively induces pulmonary vascular apoptosis and reverses pulmonary arterial hypertension. *J Clin Invest.* 2005;115(6):1479-1491.

8. Schermuly RT, Dony E, Ghofrani HA, Pullamsetti S, Savai R, Roth M, Sydykov A, Lai YJ, Weissmann N, Seeger W, Grimminger F. Reversal of experimental pulmonary hypertension by PDGF inhibition. *J Clin Invest.* 2005;115(10):2811-2821.

9. Petitjean A, Achatz MI, Borresen-Dale AL, Hainaut P, Olivier M. TP53 mutations in human cancers: functional selection and impact on cancer prognosis and outcomes. *Oncogene.* 2007;26(15):2157-2165.

10. Kubbutat MH, Jones SN, Vousden KH. Regulation of p53 stability by Mdm2. *Nature.* 1997;387(6630):299-303.

11. Mayo LD, Donner DB. The PTEN, Mdm2, p53 tumor suppressor-oncoprotein network. *Trends Biochem Sci.* 2002;27(9):462-467.

12. Vargas DA, Takahashi S, Ronai Z. Mdm2: A regulator of cell growth and death. *Adv Cancer Res.* 2003;89:1-34.

13. Vassilev LT, Vu BT, Graves B, Carvajal D, Podlaski F, Filipovic Z, Kong N, Kammlott U, Lukacs C, Klein C, Fotouhi N, Liu EA. In vivo activation of the p53 pathway by small-molecule antagonists of MDM2. *Science.* 2004;303(5659):844-848.

14. Vousden KH. Outcomes of p53 activation--spoilt for choice. *J Cell Sci.* 2006;119(Pt 24):5015-5020.

15. Alimonti A, Nardella C, Chen Z, Clohessy JG, Carracedo A, Trotman LC, Cheng K, Varmeh S, Kozma SC, Thomas G, Rosivatz E, Woscholski R, Cognetti F, Scher HI, Pandolfi PP. A novel type of cellular senescence that can be enhanced in mouse

models and human tumor xenografts to suppress prostate tumorigenesis. *J Clin Invest.* 2010;120(3):681-693.

16. Hashimoto T, Ichiki T, Ikeda J, Narabayashi E, Matsuura H, Miyazaki R, Inanaga K, Takeda K, Sunagawa K. Inhibition of MDM2 attenuates neointimal hyperplasia via suppression of vascular proliferation and inflammation. *Cardiovasc Res. 2011;* 91(4):711-719.

17. Ihling C, Haendeler J, Menzel G, Hess RD, Fraedrich G, Schaefer HE, Zeiher AM. Co-expression of p53 and MDM2 in human atherosclerosis: implications for the regulation of cellularity of atherosclerotic lesions. *J Pathol.* 1998;185(3):303-312.

18. Nakamura Y, Suzuki S, Suzuki T, Ono K, Miura I, Satoh F, Moriya T, Saito H, Yamada S, Ito S, Sasano H. MDM2: a novel mineralocorticoid-responsive gene involved in aldosterone-induced human vascular structural remodeling. *Am J Pathol.* 2006;169(2):362-371.

19. An WG, Kanekal M, Simon MC, Maltepe E, Blagosklonny MV, Neckers LM. Stabilization of wild-type p53 by hypoxia-inducible factor 1alpha. *Nature.* 1998;392(6674):405-408.

20. Efeyan A, Ortega-Molina A, Velasco-Miguel S, Herranz D, Vassilev LT, Serrano M. Induction of p53-dependent senescence by the MDM2 antagonist nutlin-3a in mouse cells of fibroblast origin. *Cancer Res.* 2007;67(15):7350-7357.

21. Kumamoto K, Spillare EA, Fujita K, Horikawa I, Yamashita T, Appella E, Nagashima M, Takenoshita S, Yokota J, Harris CC. Nutlin-3a activates p53 to both down-regulate inhibitor of growth 2 and up-regulate mir-34a, mir-34b, and mir-34c expression, and induce senescence. *Cancer Res.* 2008;68(9):3193-3203.

22. Huang B, Deo D, Xia M, Vassilev LT. Pharmacologic p53 activation blocks cell cycle progression but fails to induce senescence in epithelial cancer cells. *Mol Cancer Res.* 2009;7(9):1497-1509.

23. Miyachi M, Kakazu N, Yagyu S, Katsumi Y, Tsubai-Shimizu S, Kikuchi K, Tsuchiya K, Iehara T, Hosoi H. Restoration of p53 pathway by nutlin-3 induces cell cycle arrest and apoptosis in human rhabdomyosarcoma cells. *Clin Cancer Res.* 2009;15(12):4077-4084.

24. Noureddine H, Gary-Bobo G, Alifano M, Marcos E, Saker M, Vienney N, Amsellem V, Maitre B, Chaouat A, Chouaid C, Dubois-Rande JL, Damotte D, Adnot S. Pulmonary artery smooth muscle cell senescence is a pathogenic mechanism for pulmonary hypertension in chronic lung disease. *Circ Res.* 2011;109(5):543-553.

25. Ciuclan L, Bonneau O, Hussey M, Duggan N, Holmes AM, Good R, Stringer R, Jones P, Morrell NW, Jarai G, Walker C, Westwick J, Thomas M. A novel murine model of severe pulmonary arterial hypertension. *Am J Respir Crit Care Med.* 2011;184(10):1171-1182.

26. Guignabert C, Izikki M, Tu LI, Li Z, Zadigue P, Barlier-Mur AM, Hanoun N, Rodman D, Hamon M, Adnot S, Eddahibi S. Transgenic mice overexpressing the 5-hydroxytryptamine transporter gene in smooth muscle develop pulmonary hypertension. *Circ Res.* 2006;98(10):1323-1330.

27. Gary-Bobo G, Houssaini A, Amsellem V, Rideau D, Pacaud P, Perrin A, Bregeon J, Marcos E, Dubois-Rande JL, Sitbon O, Savale L, Adnot S. Effects of HIV protease inhibitors on progression of monocrotaline- and hypoxia-induced pulmonary hypertension in rats. *Circulation.* 2010;122(19):1937-1947.

28. Mizuno S, Bogaard HJ, Kraskauskas D, Alhussaini A, Gomez-Arroyo J, Voelkel NF, Ishizaki T. p53 Gene deficiency promotes hypoxia-induced pulmonary hypertension and vascular remodeling in mice. *Am J Physiol Lung Cell Mol Physiol.* 2011;300(5):L753-761.

29. Nardella C, Clohessy JG, Alimonti A, Pandolfi PP. Pro-senescence therapy for cancer treatment. *Nat Rev Cancer.* 2011;11(7):503-511.

30. Wade M, Wang YV, Wahl GM. The p53 orchestra: Mdm2 and Mdmx set the tone. *Trends Cell Biol.* 2010;20(5):299-309.

31. Shangary S, Qin D, McEachern D, Liu M, Miller RS, Qiu S, Nikolovska-Coleska Z, Ding K, Wang G, Chen J, Bernard D, Zhang J, Lu Y, Gu Q, Shah RB, Pienta KJ, Ling X, Kang S, Guo M, Sun Y, Yang D, Wang S. Temporal activation of p53 by a specific MDM2 inhibitor is selectively toxic to tumors and leads to complete tumor growth inhibition. *Proc Natl Acad Sci U S A.* 2008;105(10):3933-3938.

32. Lane DP, Brown CJ, Verma C, Cheok CF. New insights into p53 based therapy. *Discov Med.* 2011;12(63):107-117.

33. Wei Q, Dong G, Yang T, Megyesi J, Price PM, Dong Z. Activation and involvement of p53 in cisplatin-induced nephrotoxicity. *Am J Physiol Renal Physiol.* 2007;293(4):F1282-1291.

34. Meek DW, Knippschild U. Posttranslational modification of MDM2. *Mol Cancer Res.* 2003;1(14):1017-1026.

35. Campisi J. Senescent cells, tumor suppression, and organismal aging: good citizens, bad neighbors. *Cell.* 2005;120(4):513-522.

36. Amsellem V, Gary-Bobo G, Marcos E, Maitre B, Chaar V, Validire P, Stern JB, Noureddine H, Sapin E, Rideau D, Hue S, Le Corvoisier P, Le Gouvello S, Dubois-

Rande JL, Boczkowski J, Adnot S. Telomere Dysfunction Causes Sustained Inflammation in Chronic Obstructive Pulmonary Disease. *Am J Respir Crit Care Med.* 2011; 184(12):1358-66.

37. Baker DJ, Wijshake T, Tchkonia T, LeBrasseur NK, Childs BG, van de Sluis B, Kirkland JL, van Deursen JM. Clearance of p16Ink4a-positive senescent cells delays ageing-associated disorders. *Nature.* 2011;479(7372):232-236.

Figure 1. Effects of Nutlin-3a treatment on pulmonary-artery smooth-muscle-cells (PA-SMCs). **A**, time-dependent changes in phosphorylated p53 protein (P-p53), total p53 protein, and p53 mRNA following PA-SMC treatment with 5 µM of Nutlin-3a. **B**, changes in p21 protein and p21 mRNA following treatment with 5 µM of Nutlin-3a. **C**, percentage of beta-galactosidase-positive cells (bar graphs) and of apoptotic cells (diamonds) 24 hours after increasing doses of Nutlin-3a with or without 50 ng/mL PDGF-B. **D**, Representative photographs of cells stained for senescence-associated beta-galactosidase activity. **E**, Phosphorylated p53 (P-p53), total p53, p21, and caspase-3 protein measured by Western blot in PA-SMCs treated with increasing Nutlin-3a concentrations. Data are mean±SEM of 10 values from four independent experiments. **F,** Effects of Nutlin on firefly/renilla luciferase activity ratio in PA-SMCs co-transfected with the p53-responsive firefly luciferase construct and with a construct constitutively expressing renilla luciferase. Data are mean±SEM of 6 values. **P*<0.05; ***P*<0.01; and ****P*<0.001 compared to treatment with vehicle instead of Nutlin-3a.

Figure 2. A, right ventricular systolic pressure (RVSP); right ventricular hypertrophy index (RV/[LV+S] weight ratio); pulmonary vessel muscularization (percentages of muscularized pulmonary vessels); and percentages of Ki67-positive dividing cells, p21-stained cells, and TUNEL-positive cells in mice studied on day 21 after exposure to hypoxia or to normoxia and treated with daily i.p. injections of vehicle or various Nutlin-3a doses. **B**, representative micrographs of pulmonary vessels stained for Ki67, TUNEL, or p21. No immunoreactivity was detected in sections incubated with secondary anti-rabbit and anti-mouse antibody but no primary antibody. Data are mean±SEM of 6 to 10 animals.**P*<0.05 compared with values in vehicle-treated mice after exposure to hypoxia or normoxia. †*P*<0.05 for comparison between

hypoxic and normoxic mice treated with vehicle. **C**, RVSP, RV/[LV+S] weight ratio, and pulmonary vessel muscularization in normoxic and chronically hypoxic mice studied on day 15 and 30 after hypoxia exposure. Nutlin-3a 12 mg/Kg/d was given from day 15 to day 30. **P*<0.05 versus day 15 of hypoxia and †*P*<0.05 versus day 30 of hypoxia in vehicle-treated mice.

Figure 3. A, Lung levels of total p53 protein, p21, and MDM2 protein measured by Western blot in mice studied on day 21 after exposure to hypoxia or normoxia and treated with daily i.p. injections of vehicle or various Nutlin-3a doses. Mice were sacrificed exactly 3 hours after the last Nutlin-3a dose. **B**, p53 protein levels measured in the cytoplasmic and nuclear fractions of lung proteins and quantified relative to alpha-tubulin and lamin A/C, respectively. **C**, lung phosphorylated p53 (P-p53) levels determined using a co-immunoprecipitation procedure. **D**, lung mRNA levels of p21, bax, Bcl2, p53, PUMA and BTG2 measured by RT-PCR **P*<0.05 compared with values in vehicle-treated mice after exposure to hypoxia or normoxia. Data are mean±SEM of 6 to 10 animals. †*P*<0.05 compared with values in vehicle-treated mice after exposure to hypoxia.

Figure 4. A, right ventricular systolic pressure (RVSP); right ventricular hypertrophy index (RV/[LV+S] weight ratio); muscularization of pulmonary vessels (percentages of partially and fully muscularized pulmonary vessels); and percentages of Ki67-positive dividing cells, p21-stained cells and TUNEL-positive cells in SM22-5HTT+mice and wild-type mice studied after 21 days of treatment with vehicle or 12 mg/Kg of Nutlin-3a. **B**, representative micrographs of pulmonary vessels stained for Ki67, TUNEL, or p21. Data are mean±SEM of

6 to 10 animals.*P<0.05 compared with values in vehicle-treated mice. †P<0.05 for comparison between SM22-5HTT+ and control mice treated with vehicle.

Figure 5. Lung protein levels of p53, p21, and MDM2 measured by Western blot in SM22-5-HTT+ mice and control mice studied after 21 days of treatment with vehicle or 12 mg/Kg of Nutlin-3a. Mice were sacrificed exactly 3 hours after the last Nutlin-3a dose. Data are mean±SEM of 6 to 10 animals.*P<0.05 compared with values in vehicle-treated mice. †P<0.05 for SM22-5HTT+ versus vehicle-treated control mice.

Figure 6. Immunolocalization of MDM2 in mouse and human lung tissues. **A**, representative photographs of immunofluorescence staining for MDM2 in wild-type normoxic and hypoxic mice and in SM22-5HTT+ mice treated with Nutlin-3a or vehicle for 21 days. MDM2 was predominantly expressed in pulmonary vessels and co-localized with α-SMA in smooth muscle cells (SMCs). **B**, representative photographs of immunofluorescence staining for MDM2 in nonremodeled and remodeled vessels from lung-surgery patients. No immunoreactivity was detected in sections incubated with secondary anti-rabbit and anti-mouse antibody but no primary antibody.

Figure 7. A, right ventricular systolic pressure (RVSP), right ventricular hypertrophy index (RV/[LV+S] weight ratio), and pulmonary vessel muscularization (percentages of partially and fully muscularized pulmonary vessels); **B**, lung protein levels of p21 and MDM2 in wild-type and p53 knockout (KO) mice studied on day 21 after exposure to hypoxia or normoxia and treated with daily i.p. injections of 12 mg/Kg Nutlin-3a. Data are mean±SEM of 10

animals.*P<0.05 compared with values in vehicle-treated mice. ‡P<0.05 compared with values in vehicle-treated control mice.

Figure 8. Right ventricular systolic pressure (RVSP), right ventricular hypertrophy index (RV/[LV+S] weight ratio), pulmonary vessel muscularization (percentages of partially and fully muscularized pulmonary vessels) in wild-type and p21 knockout (KO) mice studied on day 21 after exposure to hypoxia or normoxia and treated with daily i.p. injections of 12 mg/Kg Nutlin-3a. Data are mean±SEM of 6 to 10 animals.*P<0.05 compared with values in vehicle-treated mice. ‡P<0.05 compared with values in vehicle-treated control mice.

Figure 1

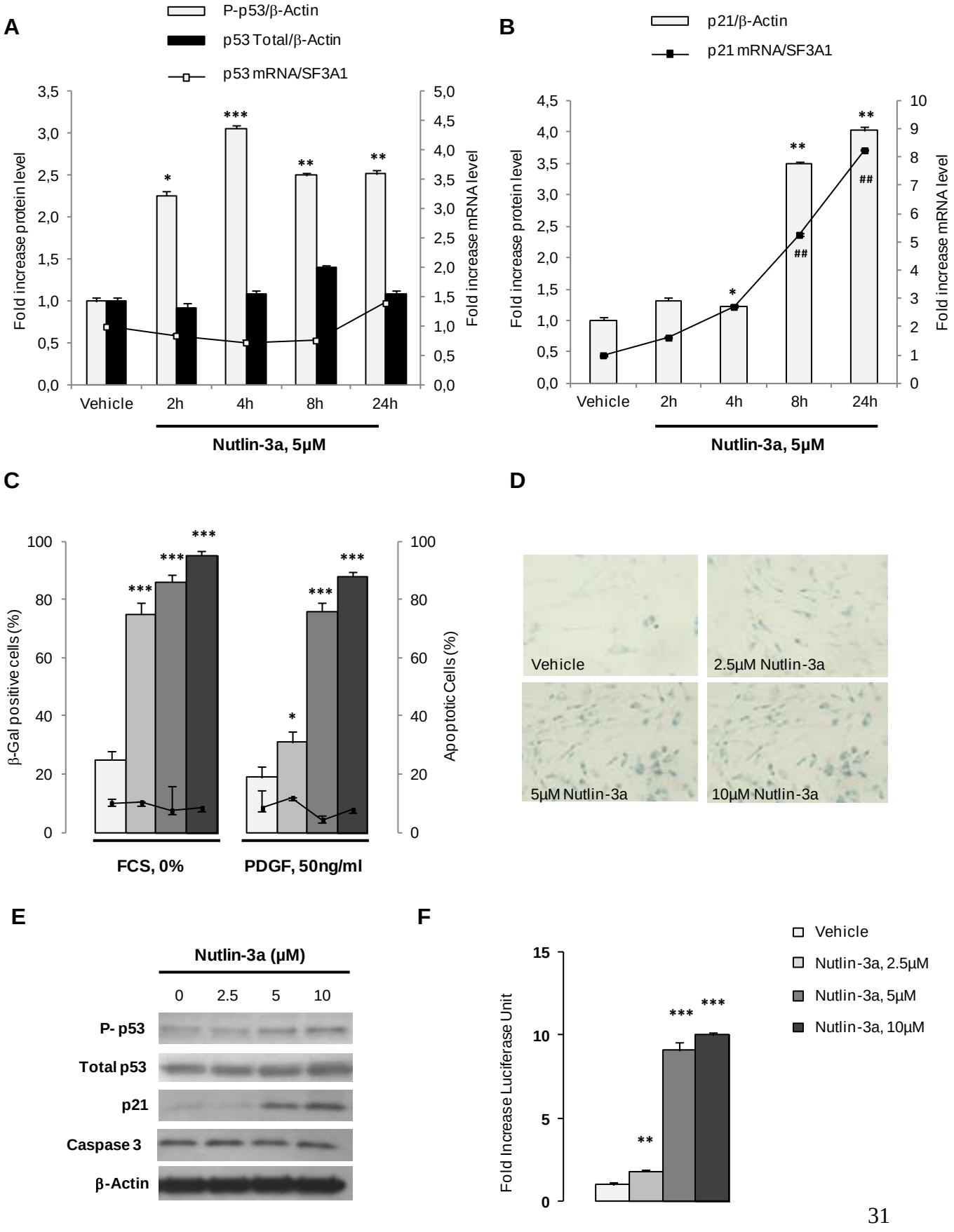
A
P-p53/β-Actin
p53 Total/β-Actin
p53 mRNA/SF3A1
Fold increase protein level
Fold increase mRNA level
Vehicle
2h
4h
8h
24h
Nutlin-3a, 5μM
B
p21/β-Actin
p21 mRNA/SF3A1
Fold increase protein level
Fold increase mRNA level
Vehicle
2h
4h
8h
24h
Nutlin-3a, 5μM
C
β-Gal positive cells (%)
Apoptotic Cells (%)
FCS, 0%
PDGF, 50ng/ml
D
Vehicle
2.5μM Nutlin-3a
5μM Nutlin-3a
10μM Nutlin-3a
E
Nutlin-3a (μM)
0
2.5
5
10
P- p53
Total p53
p21
Caspase 3
β-Actin
F
Vehicle
Nutlin-3a, 2.5μM
Nutlin-3a, 5μM
Nutlin-3a, 10μM
Fold Increase Luciferase Unit

Figure 2

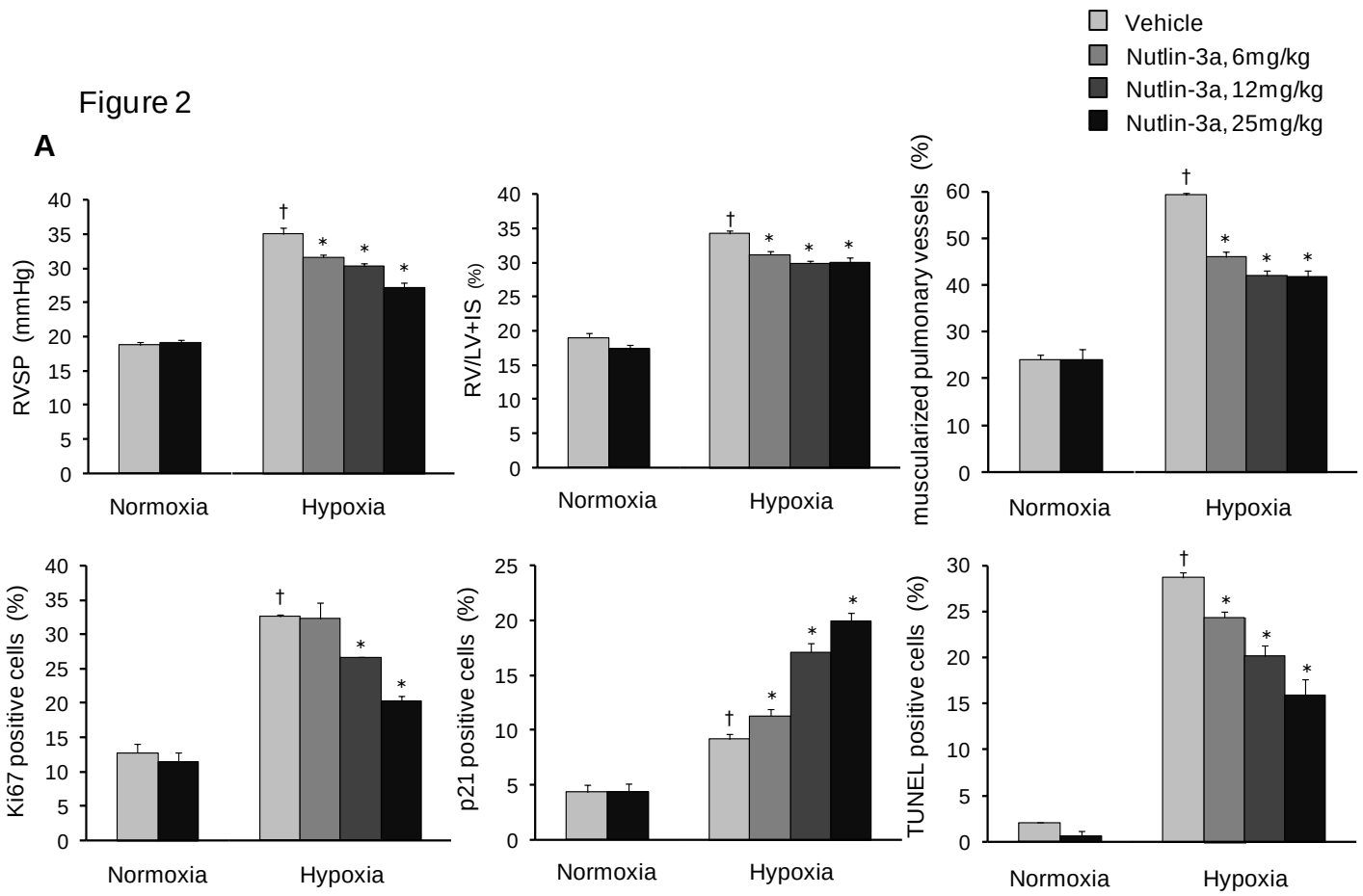
A
Vehicle
Nutlin-3a, 6mg/kg
Nutlin-3a, 12mg/kg
Nutlin-3a, 25mg/kg
RVSP (mmHg)
RV/LV+IS (%)
muscularized pulmonary vessels (%)
Ki67 positive cells (%)
p21 positive cells (%)
TUNEL positive cells (%)
Normoxia
Hypoxia

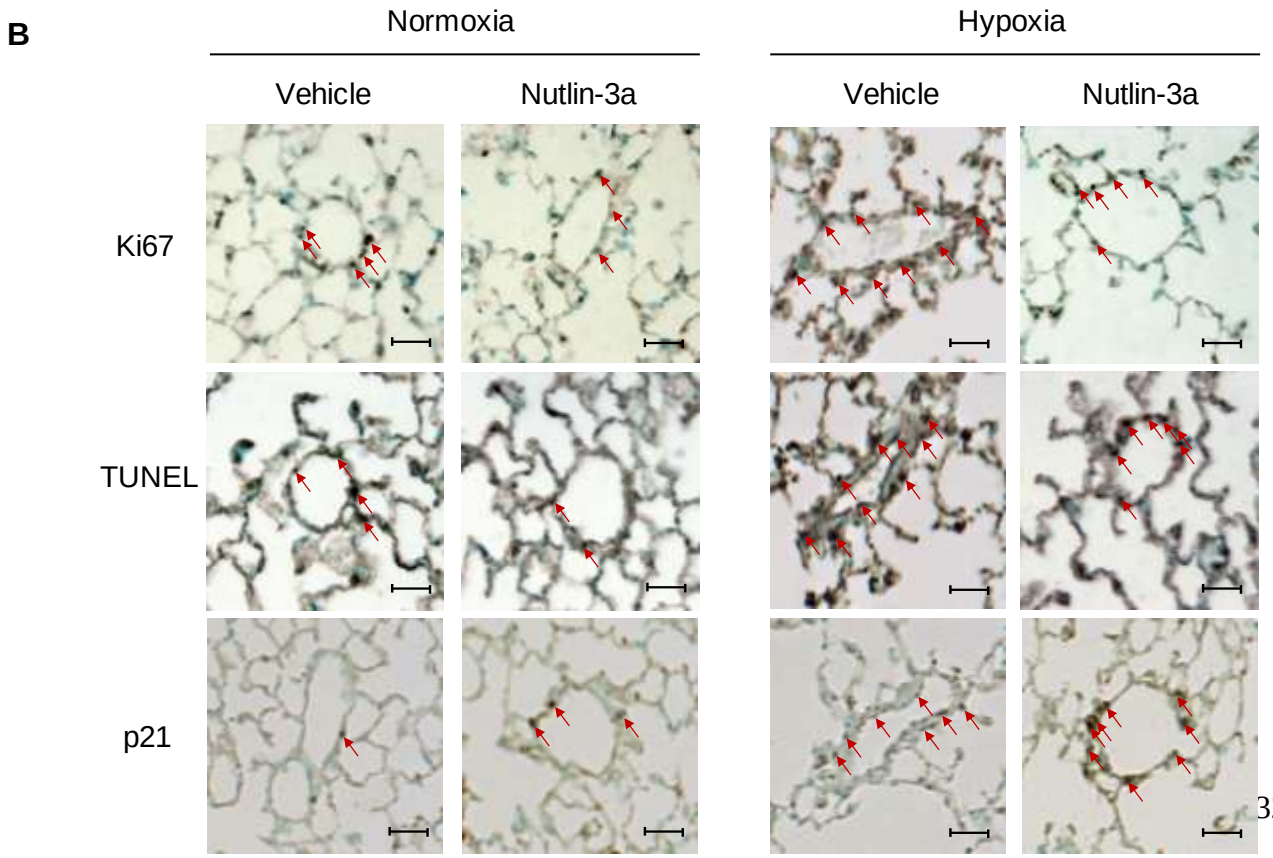
B
Normoxia
Hypoxia
Vehicle
Nutlin-3a
Ki67
TUNEL
p21

Figure 2

C

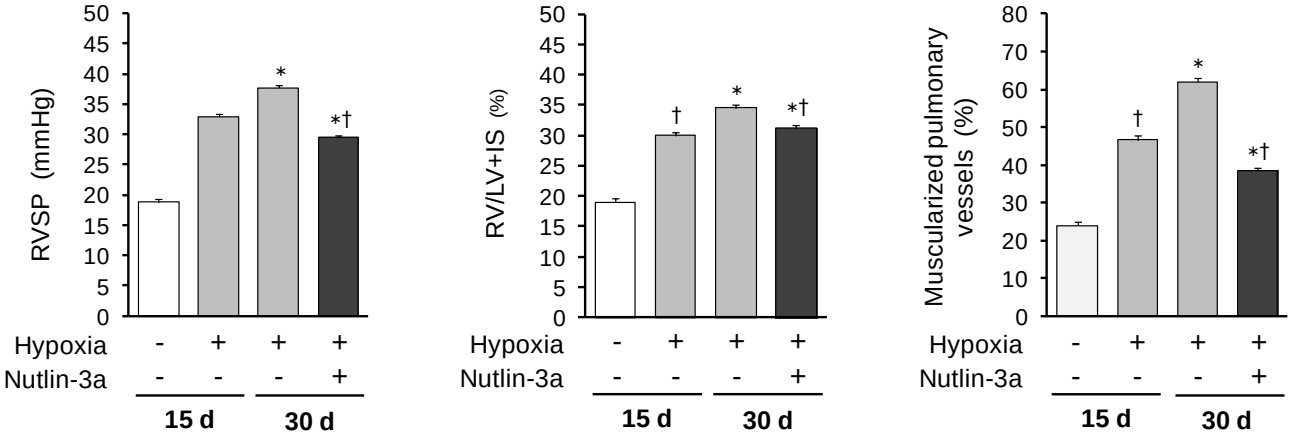
RVSP (mmHg)
50
45
40
35
30
25
20
15
10
5
0
*
*†
Hypoxia - + + +
Nutlin-3a - - - +
15 d
30 d
RV/LV+IS (%)
50
45
40
35
30
25
20
15
10
5
0
†
*
*†
Hypoxia - + + +
Nutlin-3a - - - +
15 d
30 d
Muscularized pulmonary vessels (%)
80
70
60
50
40
30
20
10
0
†
*
*†
Hypoxia - + + +
Nutlin-3a - - - +
15 d
30 d

Figure 3

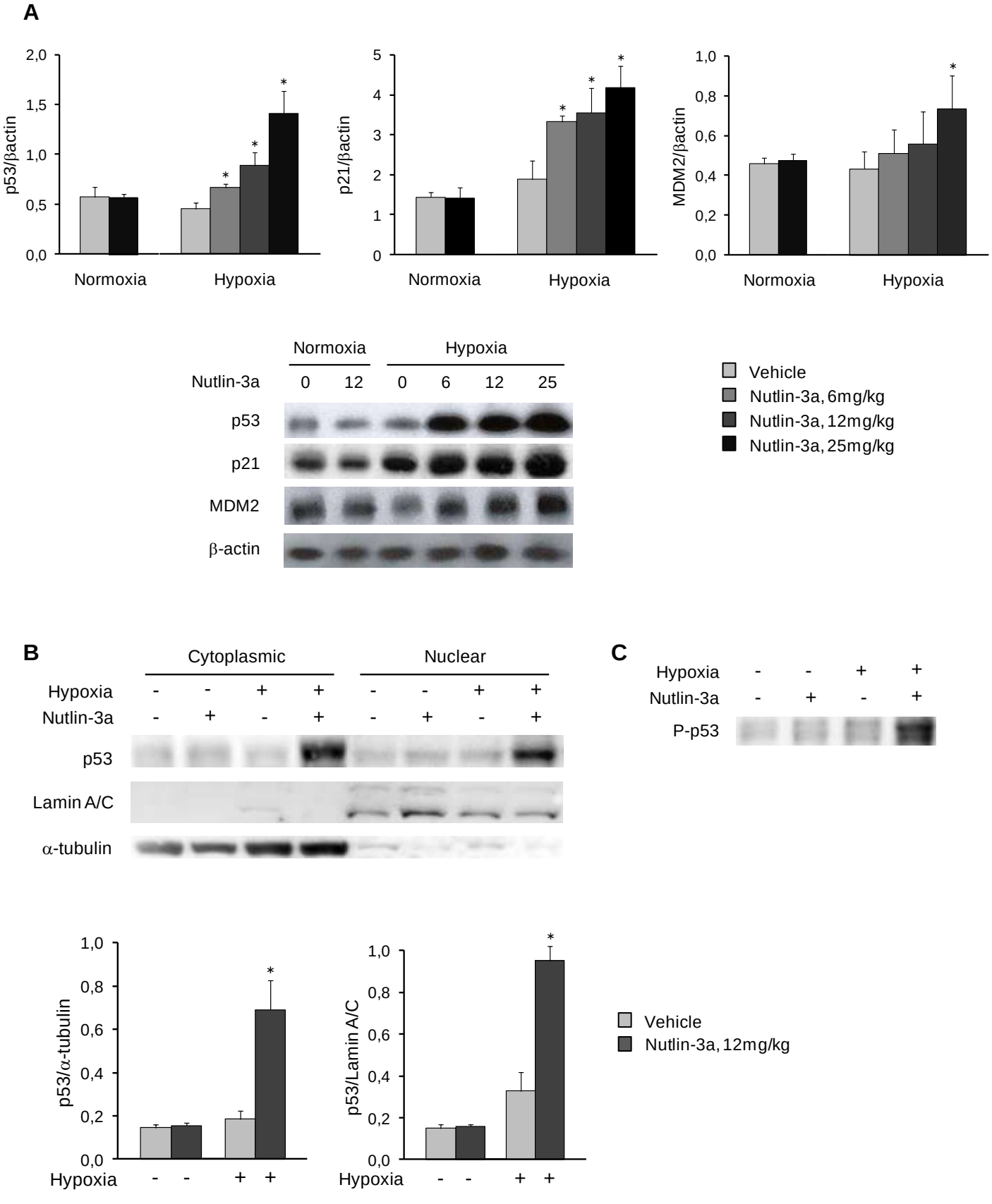
A
p53/βactin
2,0
1,5
1,0
0,5
0,0
Normoxia
Hypoxia
p21/βactin
5
4
3
2
1
0
MDM2/βactin
1,0
0,8
0,6
0,4
0,2
0,0
Normoxia
Hypoxia
Normoxia
Hypoxia
Nutlin-3a
0
12
0
6
12
25
p53
p21
MDM2
β-actin
Vehicle
Nutlin-3a, 6mg/kg
Nutlin-3a, 12mg/kg
Nutlin-3a, 25mg/kg
B
Cytoplasmic
Nuclear
Hypoxia
Nutlin-3a
p53
Lamin A/C
α-tubulin
C
Hypoxia
Nutlin-3a
P-p53
p53/α-tubulin
p53/Lamin A/C
Hypoxia
Vehicle
Nutlin-3a, 12mg/kg

Figure 3

D

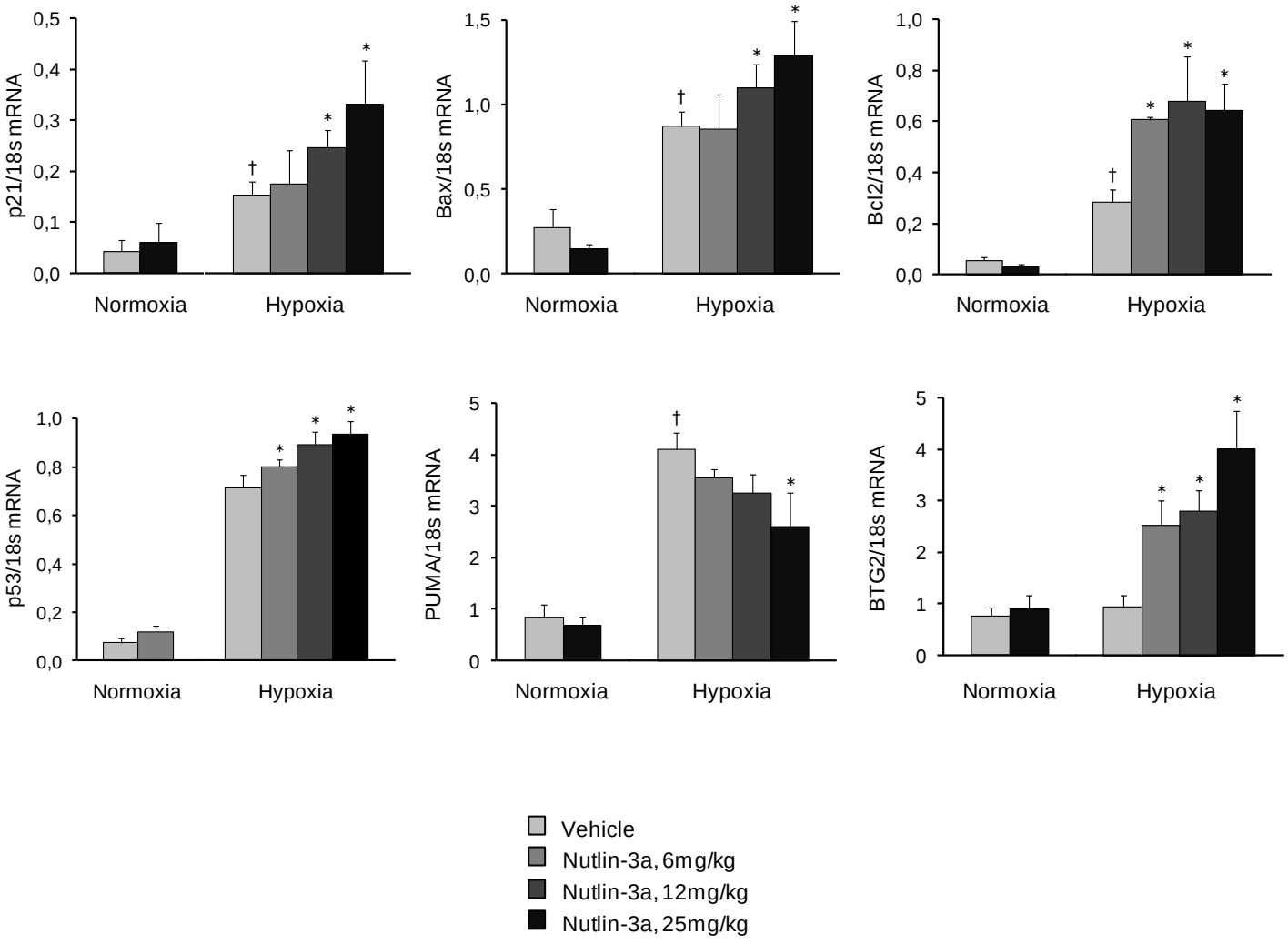
p21/18s mRNA
Bax/18s mRNA
Bcl2/18s mRNA
p53/18s mRNA
PUMA/18s mRNA
BTG2/18s mRNA
Normoxia
Hypoxia
Vehicle
Nutlin-3a, 6mg/kg
Nutlin-3a, 12mg/kg
Nutlin-3a, 25mg/kg

Figure 4

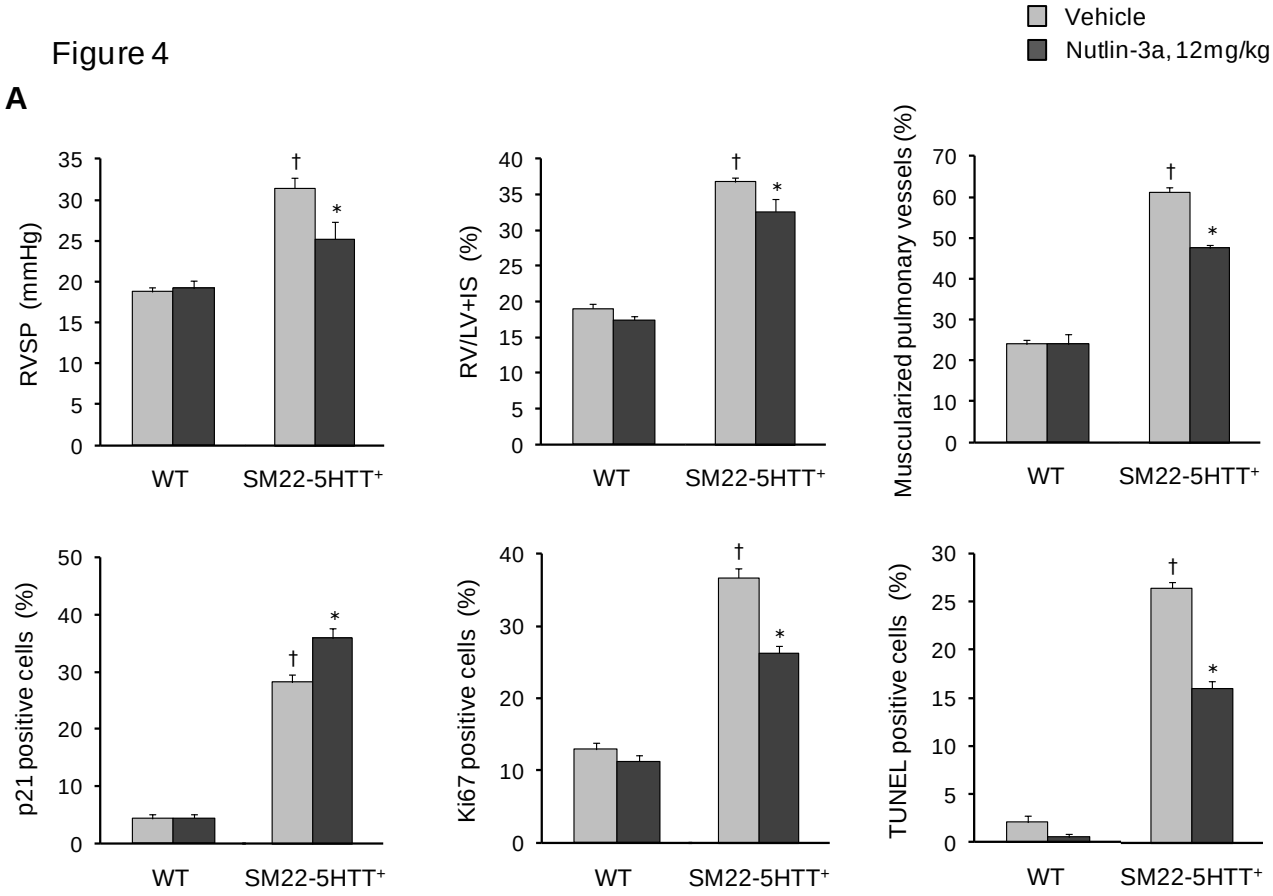
A
Vehicle
Nutlin-3a, 12mg/kg
RVSP (mmHg)
RV/LV+IS (%)
Muscularized pulmonary vessels (%)
p21 positive cells (%)
Ki67 positive cells (%)
TUNEL positive cells (%)
WT
SM22-5HTT+
†
*

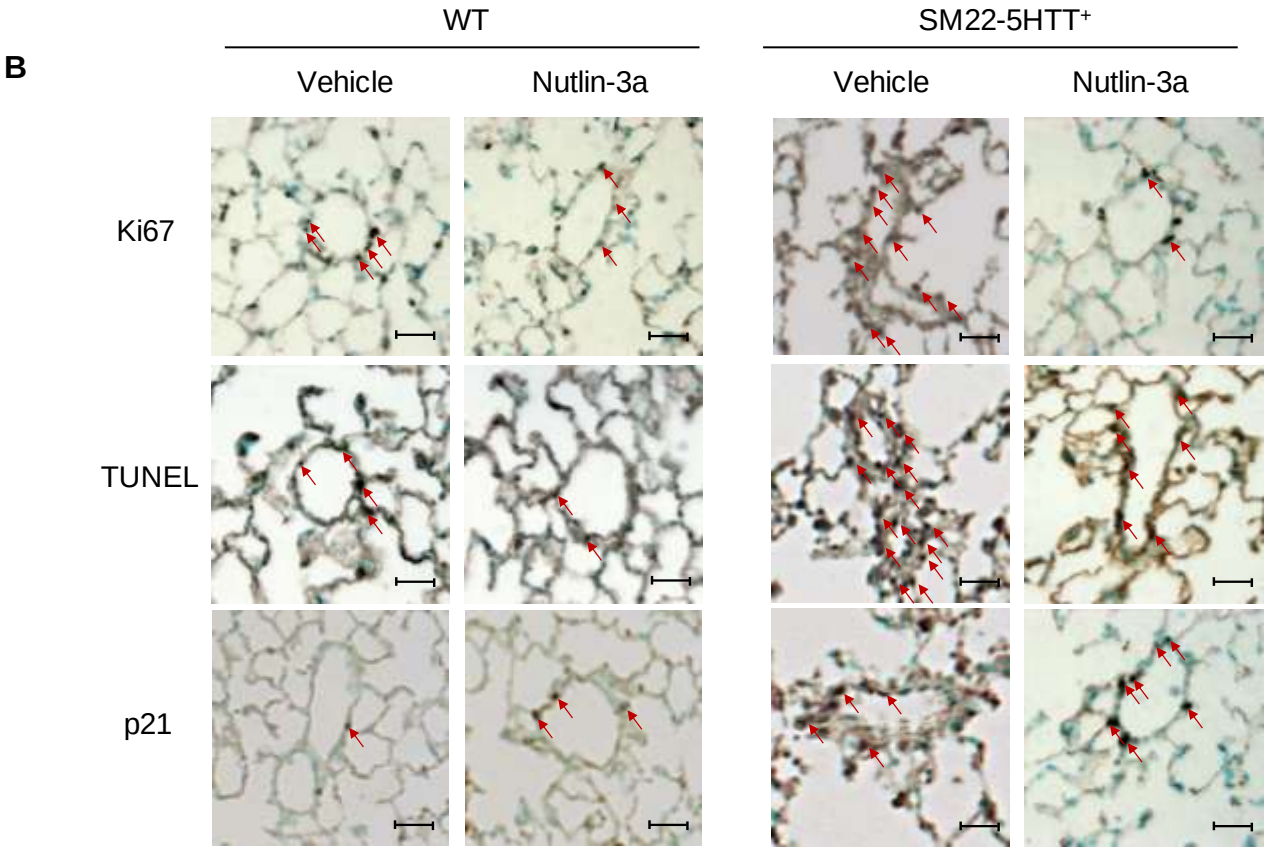
B
WT
SM22-5HTT+
Vehicle
Nutlin-3a
Ki67
TUNEL
p21

Figure 5

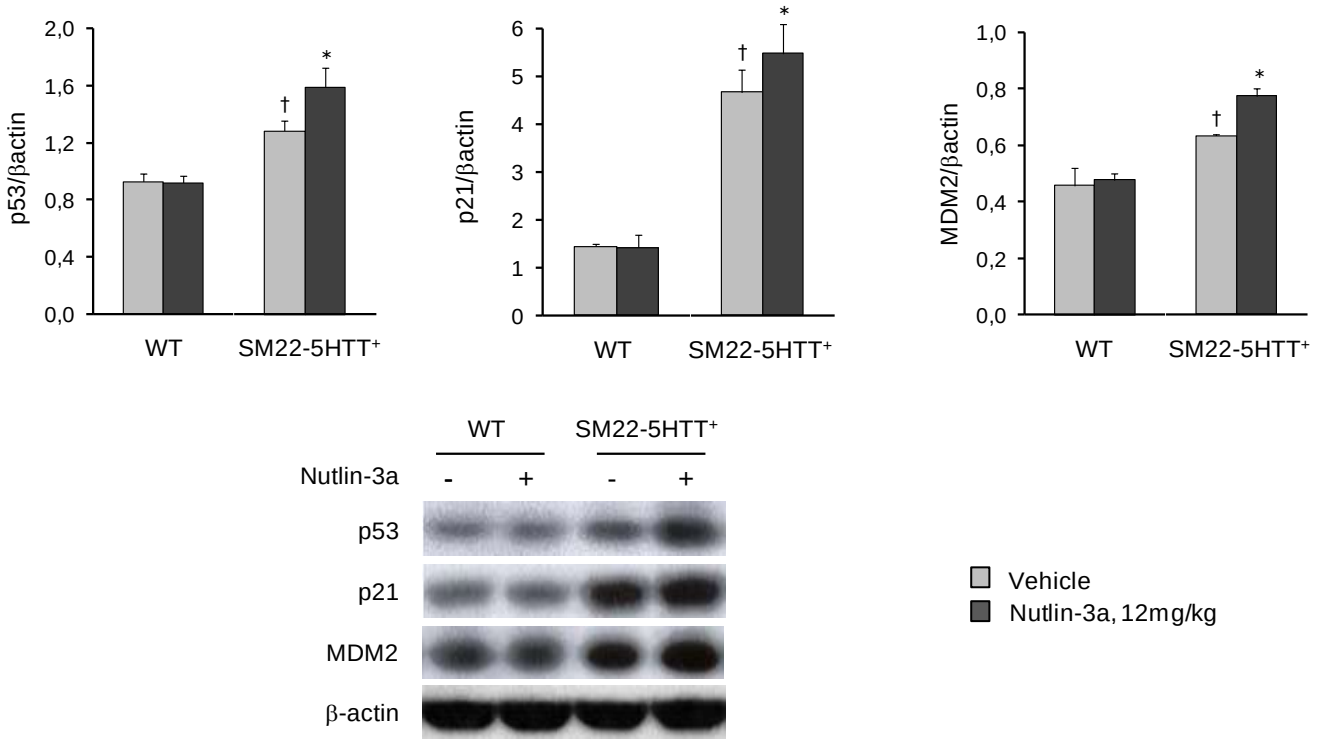
p53/βactin
2,0
1,6
1,2
0,8
0,4
0,0
†
*
WT
SM22-5HTT+
p21/βactin
6
5
4
3
2
1
0
†
*
WT
SM22-5HTT+
MDM2/βactin
1,0
0,8
0,6
0,4
0,2
0,0
†
*
WT
SM22-5HTT+
WT
SM22-5HTT+
Nutlin-3a
-
+
-
+
p53
p21
MDM2
β-actin
Vehicle
Nutlin-3a, 12mg/kg

Figure 6

A

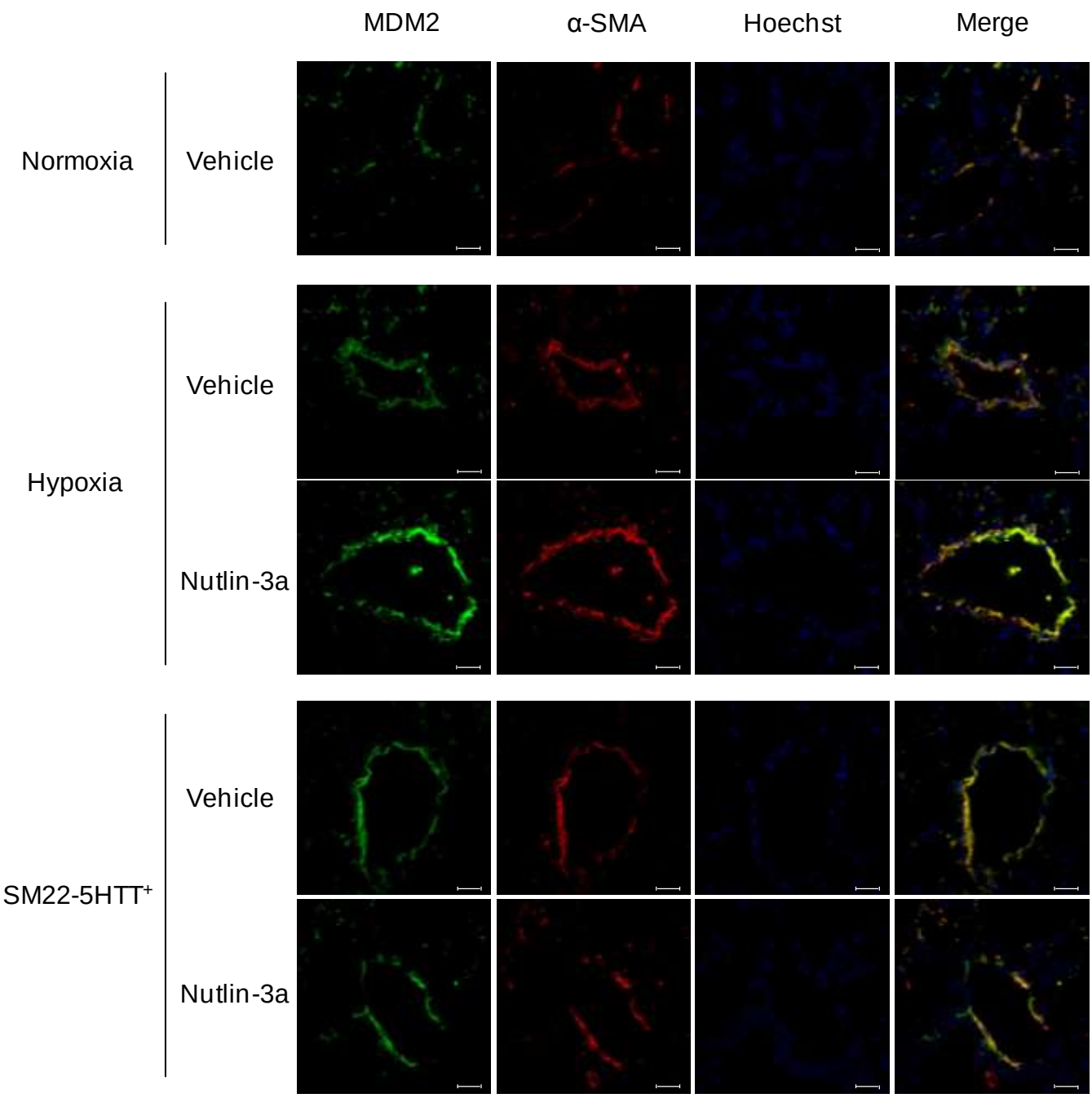
MDM2
α-SMA
Hoechst
Merge
Normoxia
Vehicle
Hypoxia
Vehicle
Nutlin-3a
SM22-5HTT+
Vehicle
Nutlin-3a

Figure 6

B

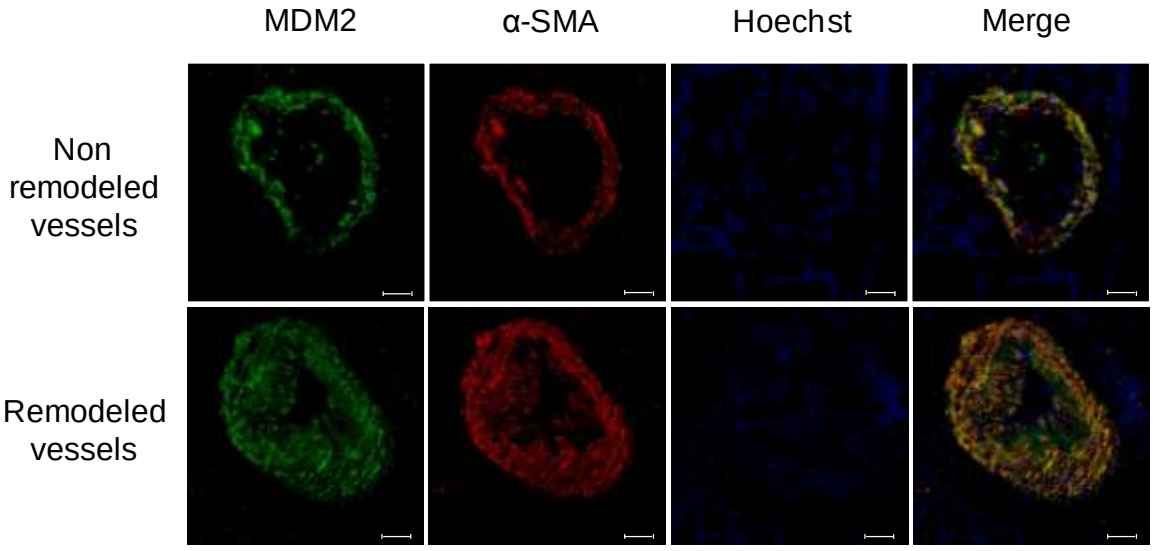
MDM2
α-SMA
Hoechst
Merge
Non remodeled vessels
Remodeled vessels

Figure 7

A

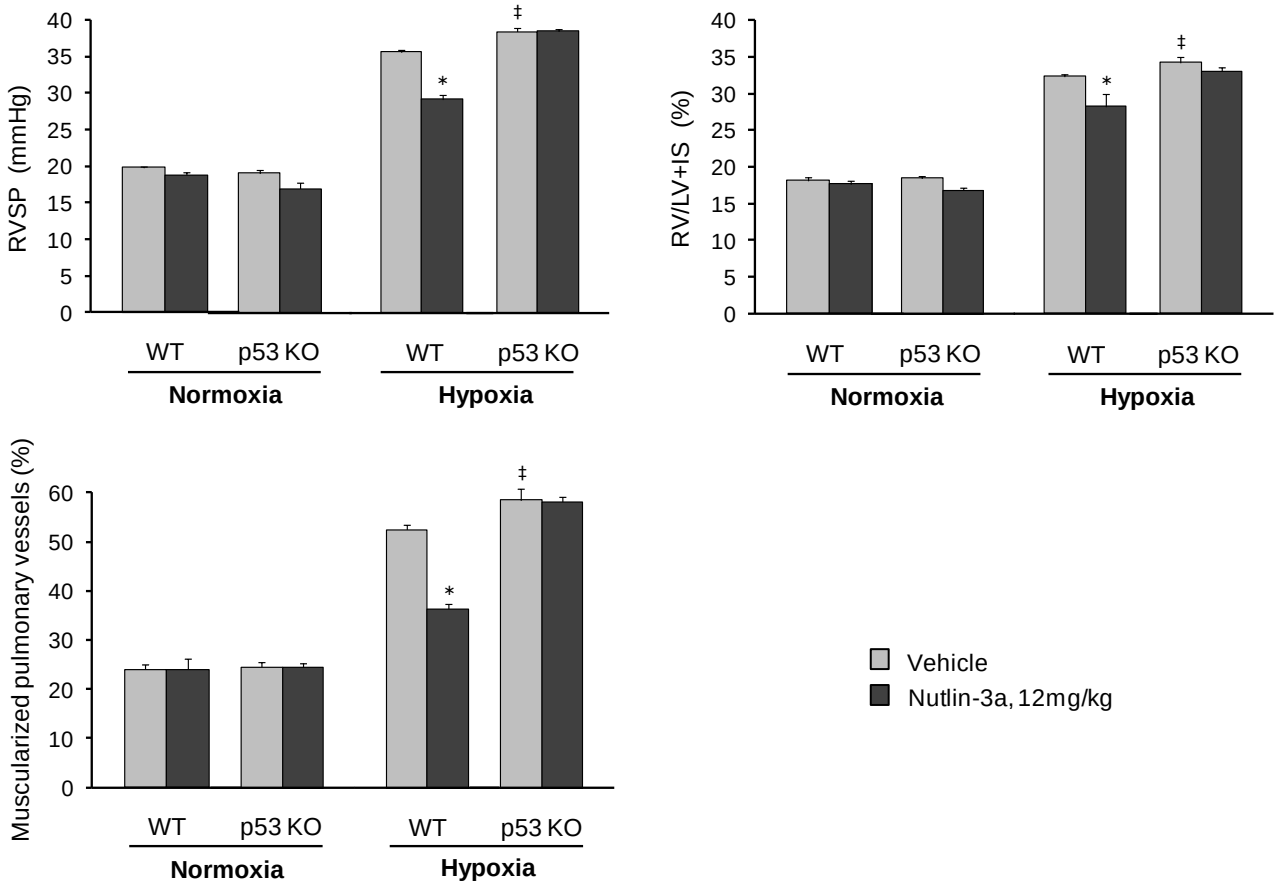
RVSP (mmHg)
RV/LV+IS (%)
Muscularized pulmonary vessels (%)
WT
p53 KO
Normoxia
Hypoxia
Vehicle
Nutlin-3a, 12mg/kg

Figure 7

B

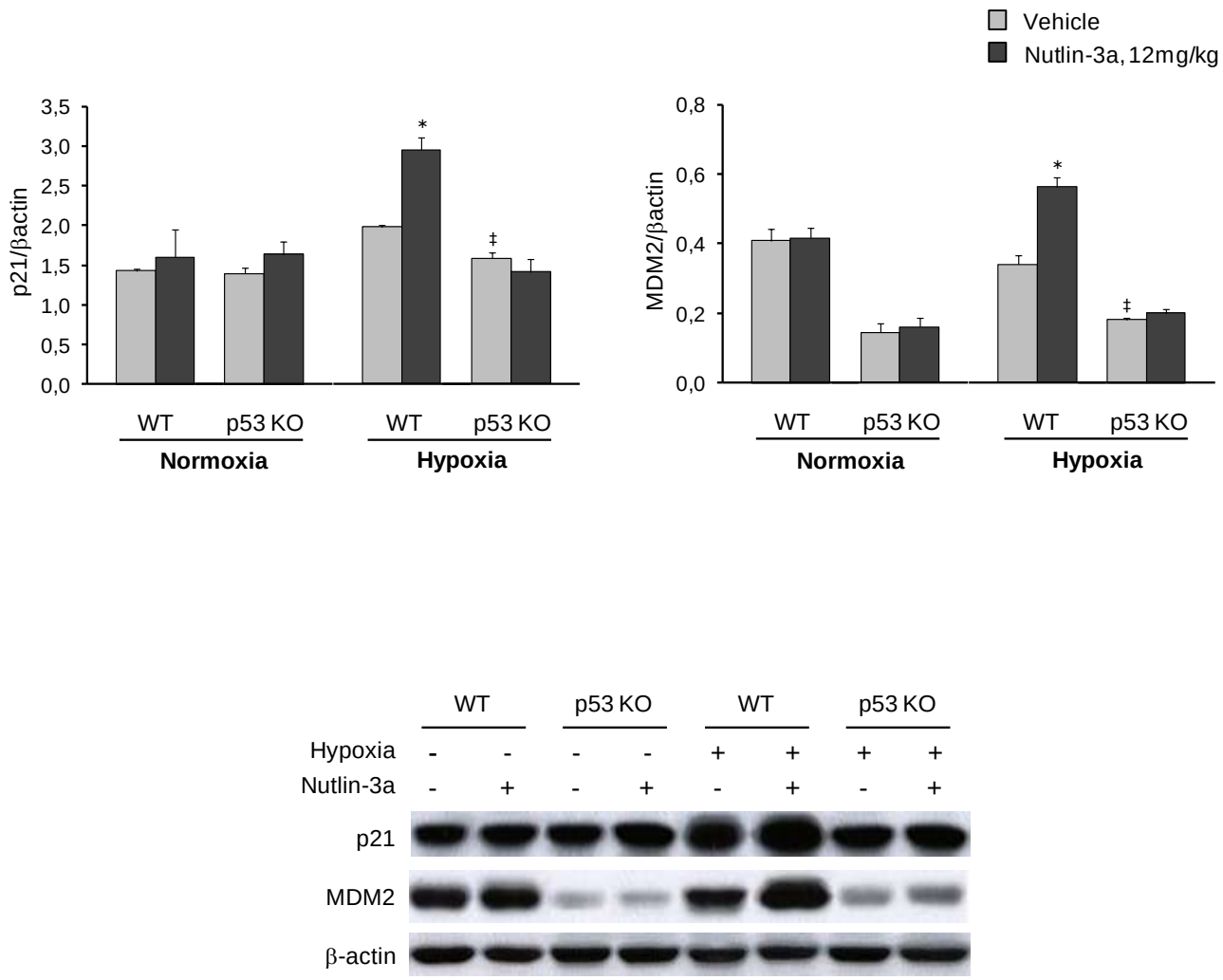
Vehicle
Nutlin-3a, 12mg/kg
p21/βactin
3,5
3,0
2,5
2,0
1,5
1,0
0,5
0,0
*
‡
WT
p53 KO
WT
p53 KO
Normoxia
Hypoxia
MDM2/βactin
0,8
0,6
0,4
0,2
0,0
*
‡
WT
p53 KO
WT
p53 KO
Normoxia
Hypoxia

WT
p53 KO
WT
p53 KO
Hypoxia - - - - + + + +
Nutlin-3a - + - + - + - +
p21
MDM2
β-actin

Figure 8

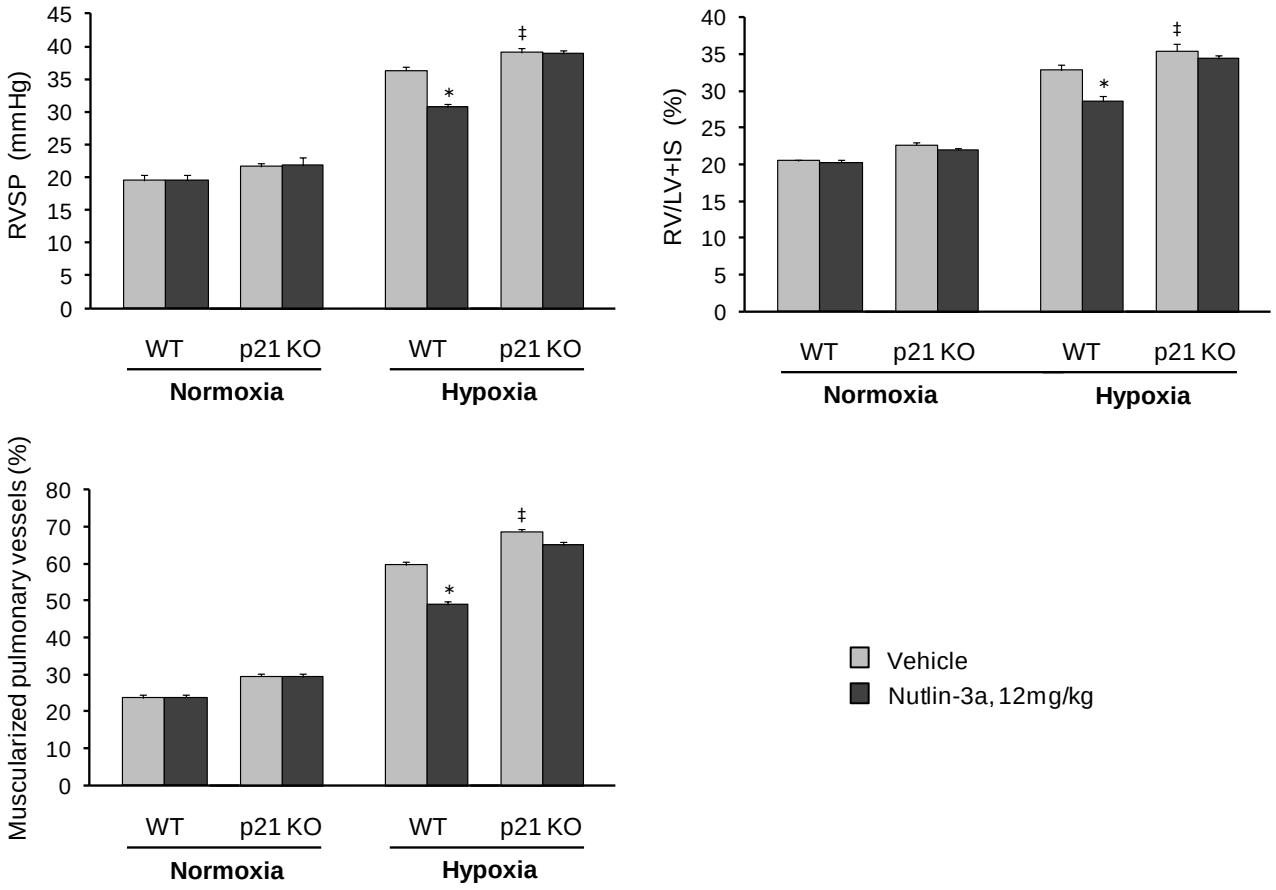
RVSP (mmHg)
45
40
35
30
25
20
15
10
5
0
*
‡
WT
p21 KO
WT
p21 KO
Normoxia
Hypoxia
RV/LV+IS (%)
40
35
30
25
20
15
10
5
0
*
‡
WT
p21 KO
WT
p21 KO
Normoxia
Hypoxia
Muscularized pulmonary vessels (%)
80
70
60
50
40
30
20
10
0
*
‡
WT
p21 KO
WT
p21 KO
Normoxia
Hypoxia
Vehicle
Nutlin-3a, 12mg/kg